Progress in PHOTOVOLTAICS

PROGRESS IN PHOTOVOLTAICS: RESEARCH AND APPLICATIONS
Prog. Photovolt: Res. Appl. 2017; **25**:41–48
Published online 5 September 2016 in Wiley Online Library (wileyonlinelibrary.com). DOI: 10.1002/pip.2808

RESEARCH ARTICLE

Economic competitiveness of III–V on silicon tandem one-sun photovoltaic solar modules in favorable future scenarios

David C. Bobela*, Lynn Gedvilas, Michael Woodhouse, Kelsey A. W. Horowitz and Paul A. Basore

National Renewable Energy Laboratory, Golden, CO, USA

ABSTRACT

Tandem modules combining a III–V top cell with a Si bottom cell offer the potential to increase the solar energy conversion efficiency of one-sun photovoltaic modules beyond 25%, while fully utilizing the global investment that has been made in Si photovoltaics manufacturing. At present, the cost of III–V cells is far too high for this approach to be competitive for one-sun terrestrial power applications. We investigated the system-level economic benefits of both GaAs/Si and InGaP/Si tandem modules in favorable future scenarios where the cost of III–V cells is substantially reduced, perhaps to less than the cost of Si cells. We found, somewhat unexpectedly, that these tandems can reduce installed system cost only when the area-related balance-of-system cost is high, such as for area-constrained residential rooftop systems in the USA. When area-related balance-of-system cost is lower, such as for utility-scale systems, the tandem module offers no benefit. This is because a system using tandem modules is more expensive than one using single-junction Si modules when III–V cells are expensive, and a system using tandem modules is more expensive than one using single-junction III–V modules when III–V cells are inexpensive. Copyright © 2016 John Wiley & Sons, Ltd.

KEYWORDS

III-V on Si; tandem solar cell; Multijunction solar cell; Balance of system costs; Total system costs

***Correspondence**

David C. Bobela, National Renewable Energy Laboratory, Golden, CO, USA.
E-mail: david.bobela@nrel.gov

Received 28 January 2016; Revised 12 July 2016; Accepted 1 August 2016

1. INTRODUCTION

In recent years, the cost of photovoltaic (PV) modules using silicon solar cells has decreased precipitously [1]. In the case of multicrystalline silicon modules, a US dollar per watt cost of $0.65/W is typical and appears to be decreasing steadily with time. Strategies for reducing this cost further typically must balance efficiency gains with an associated increase in module cost [2,3]. Combining a Si cell with one made from an epitaxial III–V material, like GaAs or InGaP, in a tandem architecture, is a heavily researched strategy for increasing the solar conversion efficiency, and cell efficiencies over 25% for one-sun terrestrial solar spectrum have recently been reported [4,5]. However, the current cost of fabricating III–V cells is more than two orders of magnitude higher than silicon, for the same area, due primarily to the high cost of the GaAs substrate and vapor-phase epitaxy [6]. As such, the III–V/Si tandem is not a cost-competitive one-sun option for the near future [7].

Assuming that the cost barrier for III–V is overcome, it is still unclear whether a tandem configuration of III–V/Si will offer a cost advantage over single-junction technologies. The tandem offers increased efficiency, but the impact on total system cost (in dollars per watt) is less obvious. When too few photons are scavenged by the bottom cell, it no longer contributes enough power to offset the cost that the bottom cell adds to the tandem structure. Moreover, the benefit of higher module efficiency on system cost depends on the specific system application. Balance-of-system (BOS) costs are dramatically different for utility or residential applications, the latter benefiting more from high-efficiency modules.

In this paper, we consider the economic competitiveness of two III–V/Si tandems, GaAs/Si, and InGaP/Si, in relation to the single-junction analogs, assuming the

aforementioned III–V cost barriers are overcome. This requires an optimization of the system cost of the tandem and then a comparison against the cost-optimized single-junction alternatives. The tandem provides a cost advantage only when its system cost is lower than both of the cost-optimized single-junction technologies.

To analyze this, we developed a simple system cost model, for one sun, fixed-tilt application, where the Si and III–V cells are equal area. This model allows for substantial future improvement in the cost of the III–V cell, while assuming that the cost of the silicon cell remains relatively fixed. Economic inputs to the model are taken from published modeling by NREL and others [2,3,6,8]. We discuss the model in Sections 2 and 3 and then explore system cost for the tandem in the context of various utility and residential-scale applications.

2. TANDEM COST MODEL

To simplify the tedious task of computing all contributions to the system cost, we have developed an analytical model that partitions the calculation into primary cost drivers that are then easily varied. A detailed analysis of system cost [8] will contain many seemingly unrelated factors; however, the factors share a commonality in that they either scale with the system's module area or with the system's power rating. For instance, a utility-scale installation of 100 MW will require an appropriately sized inverter, regardless of the module area required to achieve the system's rated power. On the other hand, costs related to racking, wiring, and conduit will scale primarily with the module area required for the installation, rather than with the power. Hence, at a high level, the system cost can be divided into area-related and power-related terms,

$$\text{System cost}\left(\frac{\$}{\text{W}}\right) = \frac{\text{Area-related costs}\left(\frac{\$}{\text{m}^2}\right)}{\text{Efficiency*1000}\ \left(\frac{\text{W}}{\text{m}^2}\right)} + \text{Power-related costs}\ (\$/\text{W}), \quad (1)$$

where "efficiency" refers to the module's total-area rated power conversion efficiency. If the system cost structure is known, then each cost factor can be binned as either a power-related or area-related BOS cost. Using 2015 fixed-tilt utility and area-constrained residential data from Jones-Albertus *et al.* [8] as a template for the cost structure, we binned the different factors, according to their importance in the application, into area and power terms as listed in Tables I and II. We assume that the application determines how the factor scales and in doing so, we likely approximate the reality that some costs are a function of both power and area. To represent area-related costs in $\$/m^2$, we scaled Jones-Albertus' data by the power generated per m^2 using their assumptions of either 16% or 20% efficient silicon module for today's estimates and 2020 SunShot targets, respectively. By summing the costs in each bin, we derive power-related and area-related balance of systems parameters, BOS_P and BOS_A, respectively, which capture all non-module-related costs. This two-parameter approach offers more transparency than single-parameter BOS definitions (see *SunShot Vision Study* [9], for instance) in evaluating how an improvement to BOS, cell assembly, or cell cost impacts the system cost.

We account for cell-level fabrication costs and module assembly costs separately, because cell costs may vary in a tandem module (for example, due to adjustment of layer thicknesses or future technology improvements), whereas module assembly costs will remain essentially unchanged. The cell thickness affects both the cell fabrication cost and the module efficiency, so the net impact on the system cost is nontrivial. Costs involved in module assembly can be inferred from well understood and vetted cost models for traditional Al-BSF type silicon modules [3] and are not expected to vary significantly in the future for modules of similar size and complexity.

Inserting these terms into Equation (1), the equation takes a form that shows the explicit dependences of system cost (in \$/W) on cell cost (in $\$/m^2$), including each term described earlier,

Table I. Detailed cost structure of power-related and area-related BOS factors for the utility scale, fixed-tilt installation.

Power-related cost factor	Cost (\$/W) (Ref [8])		Area-related cost factor	Cost ($\$/m^2$) (Ref [8])	
	2015	SunShot		2015	SunShot
Inverter	0.15	0.1	BOS equipment	56	50
Grid interconnection	0.05	0.03	Installation labor	32	20
Permitting	0.03	0.03	Land cost	5	6
Customer acquisition and system design	0.02	0.01			
Installer overhead and profit	0.2	0.1			
Sales tax	0.05	0.05			
Total BOS_P (\$/W)	0.50	0.32	Total BOS_A ($\$/m^2$)	93	76

Data are taken from Jones-Albertus *et al* [8]. Area-related cost factors are scaled by the power generated per m^2 assuming a 16% efficient module for 2015, and a 20% efficient module for SunShot targets. The resulting power-related and area-related balance-of-system terms relevant to our model (BOS_P and BOS_A, respectively) are shown in the last row.

BOS, balance-of-system.

DOI: 10.1002/pip

Table II. Cost structure of power-related and area-related BOS factors for the area-constrained residential-scale installation using data from Jones-Albertus *et al* [8].

Power-related cost factor	Cost ($/W) (Ref [8])		Area-related cost factor	Cost ($/m^2) (Ref [8])	
	2015	SunShot		2015	SunShot
Inverter	0.3	0.15	BOS equipment	80	60
Sales tax	0.1	0.05	Installation labor	56	30
			Permitting	16	10
			Customer acquisition and system design	56	20
			Installation overhead and profit	112	40
Total BOS_P ($/W)	0.4	0.2	Total BOS_A ($/m^2)	320	160

Area-related cost factors are scaled by the power generated per m^2 assuming a 16% efficient module for 2015 and a 20% efficient module for SunShot targets. The resulting power-related and area-related balance-of-system terms relevant to our model (BOS_P and BOS_A, respectively) are shown in the last row.

BOS, balance-of-system.

$$\begin{aligned}&\text{System costs}\,(d_{\text{III–V}}, d_{Si}, BCC_{\text{III–V}}) \\ &= \frac{[\text{Cell cost}(d_{\text{III–V}}, d_{Si}, BCC_{\text{III–V}}) + \text{Module assembly} + BOS_A]}{\eta(d_{\text{III–V}}, d_{Si})*1000} \\ &\quad + BOS_P,\end{aligned} \tag{2}$$

where d denotes the cell thickness, η represents the module efficiency, and BCC represents "base cell cost," which is explained later. For clarity, we indicate the explicit model dependence on variables bound by parentheses. We view the general utility of Equation (2) optimal when significant uncertainty exists for the cost of one technology in the tandem compared with the other. Then, the model is most sensitive to only those few parameters related to the uncertain component, and general cost trajectories can be calculated without regard for exactly how the cost reduction for the uncertain component may be realized. For III–V/Si tandems, the III–V component represents the lion's share of the cost today and the major uncertainty in the future cost of the tandem. Equation (2) lets us explore how system cost will vary as the BCC of the III–V cell is substantially reduced in the future.

In Equation (2), the cell cost function captures costs related to fabricating the operating PV cell of some thickness, d. We implement a simple cost function that takes a "base cell cost," BCC, which represents the cost of fabricating a cell of a given technology of a given thickness, and then either adds or subtracts an amount to adjust for any deviation in cell thickness. As long as the sensitivity of cell cost to cell thickness is reasonably well understood, the cell cost function (in $/m^2) takes the form,

$$\text{Cell cost}(d, BCC) = BCC + \frac{\partial(BCC)}{\partial d}(d - BCT) \tag{3}$$

where $\frac{\partial(BCC)}{\partial d}$ (in $/m^2/μm) represents the change in cell cost per unit thickness, and BCT is the base cell thickness. Costs for PERC silicon technology with $BCT = 180\,\mu m$ are well understood, as are the dependence of the cell cost on wafer thickness [2,3,10,11]. These terms are likely to be stable in coming years, given the maturity of Si technology.

In contrast, little is known about the future of III–V cells. We take the III–V BCC as a free parameter, subject to future reduction. The remaining unknown is the sensitivity of III–V cell cost to the III–V cell thickness. The III–V cell's cost dependence on thickness is inherently tied to the cost of III–V epitaxial deposition and will therefore benefit from any future reduction in the deposition cost. We therefore choose to allow the dependence of cell cost on cell thickness to scale with the III–V BCC. At any point in time, the cost of the device-layer epitaxy will account for some fraction of the total cell cost, which we call FC_{epi}. Using the single-junction GaAs cost model developed at NREL [6], we infer FC_{epi} to be about 25%. Hence, for a hypothetical 2-μm GaAs cell that costs $100/m^2, changing the device thickness from 2 μm would change the cost by ($100/m^2/2 μm) × (0.25) = $12.5/m^2/μm. We summarize these cost sensitivity terms in Equation (4a) and (4b).

$$\frac{\partial(BCC)}{\partial d} = 0.1\,\frac{\$}{\text{m}^2\cdot\mu\text{m}}\ \text{(for silicon)} \tag{4a}$$

$$\begin{aligned}\frac{\partial(BCC)}{\partial d} &= FC_{epi}*\frac{BCC}{BCT} \\ &= 0.25*\frac{BCC}{BCT}\ \frac{\$}{\text{m}^2\cdot\mu\text{m}}\ \text{(for III–IV)}\end{aligned} \tag{4b}$$

Table III contains the parameter definitions along with units and values used in our model for the installed cost of PV systems incorporating III–V/Si tandem modules.

3. TANDEM PERFORMANCE MODEL

We simulated device performance for Si and GaAs single-junction cells as well as for GaAs/Si and InGaP/Si tandem structures using PC1D [12]. For the III–V top cell, we created individual models representative of best-in-class

Table III. List of parameters used in cost model equations.

Parameter	Description, unit	Value	
		Silicon	III–V top cell
d_{III-V}, d_{Si}	Cell thickness, μm	Variable	Variable
BCC	Base cell costs, $/m^2	70	Variable
BCT	Base cell thickness,μm	180	2
η	Module efficiency	Computed using PC1D	
$\frac{\partial(BCC)}{\partial d}$	Change in cell cost per unit thickness, $/m^2/μm	0.1	$FC_{epi}\ \frac{BCC}{BCT} = 0.25 * \frac{BCT}{2}$
FC_{epi}	Fraction of cell cost related to epitaxy at 2 μm	Does not apply	0.25
Module assembly	Cost related to build-out of module, $/m^2	40—single junction 45—tandem configuration	
		Utility scale (not area-constrained)	Residential scale (area-constrained)
BoS_A	Area-related balance-of-system costs, $/m^2	93—2015 76—SunShot	320—2015 160—SunShot
BoS_P	Power-related balance-of-system costs, $/W	0.5—2015 0.32—SunShot	0.4—2015 0.2—SunShot

published devices that matched published EQE, Voc, and FF data [4,13–15]. The modeled performance of the 2-μm GaAs top cell, at base cell thickness under one-sun AM1.5G spectrum at 25 °C, is Voc = 1093 mV, Jsc = 28.9 mA/cm^2, and η = 27.9%. The corresponding performance of a 1 μm $In_{0.5}Ga_{0.5}P$ top cell is Voc = 1436 mV, Jsc = 16.4 mA/cm^2, and η = 20.4.

A high-quality 180-μm PERC silicon cell model was used for the bottom cell, which gives, under one-sun AM1.5G spectrum at 25 °C, Voc = 645 mV, Jsc = 38.5 mA/cm^2, and η = 20.6%.

To compute the tandem efficiency, we first computed top cell efficiency versus thicknesses under one-sun AM1.5G spectrum. The light not absorbed in the top cell was then passed to the Si bottom cell without optical loss. This assumes that the top cell is designed so that its efficiency is not reduced as a result of making its rear surface optically transparent, which could be technically challenging. Recent InGaP/Si mechanical stacking efforts, however, have shown encouraging progress towards 30% devices with good current collection from the bottom silicon cell [4]. We computed the tandem efficiency for a range of thicknesses for the top and bottom cells using the tandem-cell method recommended on the PC1D/PC2D website [16].

To emphasize best tandem efficiencies, we assume a four-terminal configuration, whereby the total efficiency is the sum of the top and bottom cell efficiencies. This would in practice be implemented as a voltage-matched parallel connection at the module level, and we add $5/m^2 to the module assembly cost to account for the added interconnect complexity. Where practical, we also consider a two-terminal current-matched configuration representative of a monolithically grown III–V/Si architecture and assume no change in the module assembly cost for this configuration. To account for module-related efficiency losses (inactive perimeter, interconnect losses, mismatch, glass reflectance, etc.), we multiply the calculated cell efficiency by 0.9 to obtain the module efficiency, for both tandem and single-junction configurations [3].

Because cell thickness affects cell cost, application of Equations (2)–4 is most straightforward when the tandem efficiency is plotted as a function of both top and bottom cell thickness, as shown in Figure 1. Although InGaP offers a near-ideal bandgap pairing with Si, the peak efficiency of the InGaP/Si tandem is no higher than for the GaAs/Si tandem because the electronic quality of the InGaP material inferred from the performance of the best-in-class devices is not as good as for GaAs.

We can now combine this performance model with the cost model of Section 2 to explore trajectories of future reduction in III–V BCC that could lead to a lower cost for tandem modules than for either of the single-junction alternatives. We first examine GaAs/PERC Si, then InGaP/PERC Si.

4. GaAs/PERC Si TANDEM

As a first demonstration of the system cost model, we compare the system costs of a cost optimized GaAs/PERC Si against the best cost single-junction alternatives, using GaAs BCC as the free variable. The three system cost curves using the utility scale BOS parameters for 2015 are shown in Figure 2. Importantly, these data are generated by selecting the thickness combination that minimizes system cost ($/W), which may be different than the combination maximizing efficiency. The tandem offers a cost advantage over Si for GaAs BCC costs from $0 to $125/m^2. Between $125 and $175/m^2, there is no cost advantage, while above $175/m^2, the tandem provides an advantage over GaAs. However for this utility scale scenario (where the areal costs are smaller than space constrained applications), the tandem system costs never enters the hatched region where there is cost advantages over both single-junction alternatives.

DOI: 10.1002/pip

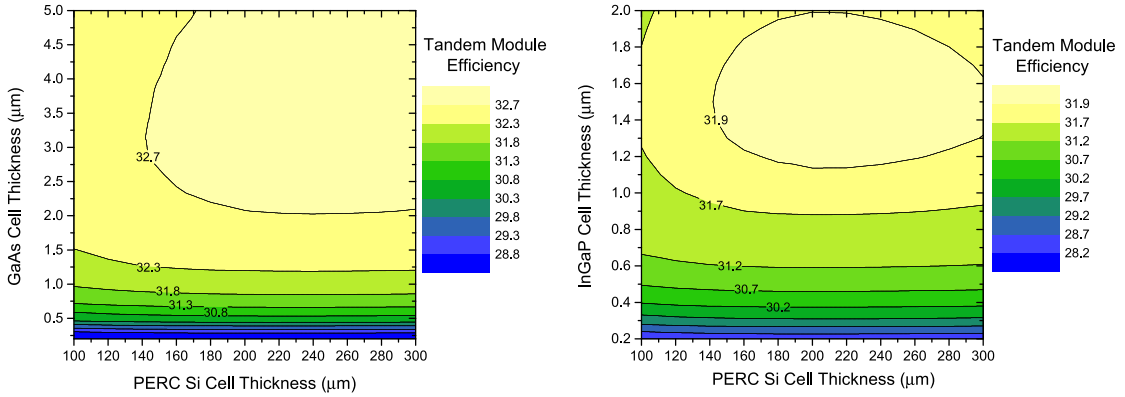

Figure 1. Four-terminal tandem cell efficiency versus cell thickness calculated using PC1D for GaAs/PERC Si (left), InGaP/PERC Si (right).

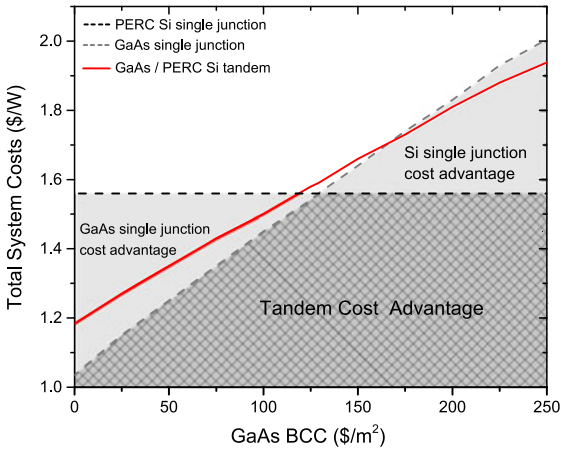

Figure 2. Total system cost for a GaAs/PERC Si tandem module, compared against the GaAs and PERC Si single-junction costs, as GaAs base cell cost (BCC) costs decrease. Data use 2015 utility scale BOS parameters. For these parameters, the tandem never offers a cost advantage over both single-junction alternatives, regardless of GaAs BCC.

While it is useful to consider single scenarios graphically as shown in Figure 2, comparing multiple scenarios on one graph becomes cumbersome. When comparing tandem modules to the single-junction alternatives, a particularly useful way to visualize a wide range of BOS scenarios across a wide range of BCC is to calculate the ratio of tandem-optimized system cost ($/W) to the single-junction-optimized system cost ($/W) for each of the two single-junction alternatives, and plot this parametrically using the III–V top-cell BCC as the free variable. Results using this methodology are shown in Figures 3 and 4. In Figure 3(a), the black squares correspond to the data in Figure 2. When the tandem/single-junction ratio is below 1, the tandem offers a cost advantage. Hence, in this parametrized plot, the cost-competitive region like that represented by the hatched region in Figure 2 is always defined by the area from (0,0) to (1,1), (the unit quadrant). The entry/exit points from this quadrant bracket the range of BCC values where the tandem is preferred over both single-junction alternatives.

Shown in Figure 3(a) are the normalized cost trajectories for the GaAs/Si tandem using utility-scale and residential-scale BOS parameters from Table III, based on today's cost estimates and 2020 SunShot targets.

For both utility-scale scenarios (black curves), the trajectories remain outside the cost-competitive region, meaning that no matter what the cost of GaAs cells may be, the tandem is more expensive at system level than either Si alone (when GaAs is expensive) or GaAs alone (when GaAs is inexpensive). Trajectories for residential applications indicate that some scenarios are cost-competitive. For a space-constrained residential system, the high area-related costs are reflected in the large BOS_A term, and hence, for today's cost (blue squares), the GaAs/Si tandem enters the cost-competitive region when GaAs base cell cost dips below $\$260/m^2$. The trajectory remains competitive, even when the base cell cost approaches $\$0/m^2$ (free GaAs cell). If SunShot BOS targets are achieved, the trajectory shifts upward and decreases the benefit of a GaAs/Si tandem. Although the analysis indicates a broad window of opportunity for GaAs/Si in today's space-constrained residential systems, the cost advantage afforded by this technology over the single-junction alternatives is at most 6.5%.

So far, we have only considered the four-terminal tandem configuration because, conceptually, it affords the most flexibility to achieve maximum efficiency. However, monolithic growth of GaAs on a silicon template is one well-researched strategy for achieving the tandem configuration, and in that structure, current matching is required by the topology to achieve competitive tandem efficiency. The current matched configuration therefore leads to a lower current, higher voltage module with respect to the voltage matched, or four-terminal options. As a result, it may offer cost advantages at the module assembly level by, for

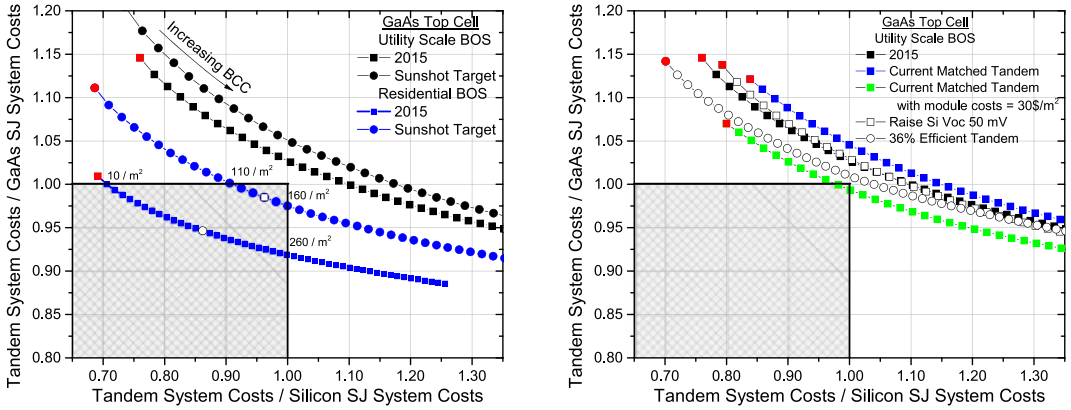

Figure 3. Total system cost for a GaAs/Si tandem, as GaAs base cell cost (BCC) cost decreases. Lines are aids to the eye. Data colored red denote where BCC = \$0/m^2. Curves are normalized to the optimized single-junction system cost using either PERC Si alone (*x*-axis) or GaAs alone (*y*-axis). BCC values for entry and exit points into the unit quadrant are noted. (a) Comparison of trajectories for residential and utility balance-of-system (BOS), using estimates of 2015 values and SunShot targets found in Table III. At the open square and open circle, GaAs and Si thicknesses are 1.3 and 100 µm, and 1.0 and 100 µm, respectively. (b) Cost trajectories showing the impact of imposing current matching, increasing the silicon bottom cell efficiency by increasing its voltage, or increasing the tandem module efficiency to 36%.

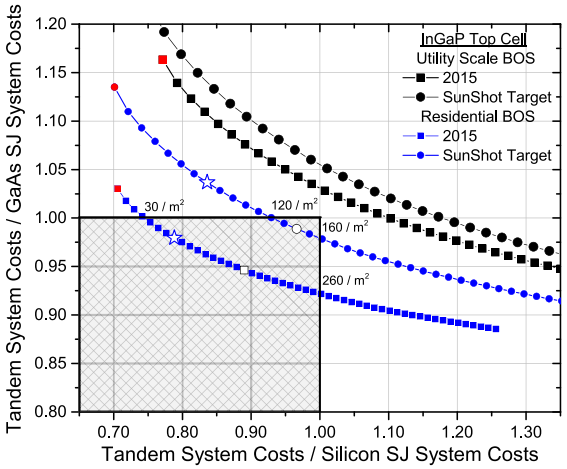

Figure 4. System cost for an InGaP/Si tandem, as InGaP base cell cost (BCC) costs decrease. Lines are aids to the eye. Data colored red denote where BCC = \$0/m^2. Curves are normalized to the optimized single-junction system cost using either Si only (*x*-axis) or GaAs only (*y*-axis). Stars indicate points where InGaP BCC = Si BCC (\$70/m^2). At the open square and open circle, InGaP and Si thicknesses are 0.8 and 100 µm, respectively. BCC values for entry and exit points into the unit quadrant are noted.

instance, reducing the amount of metal used in cell tabbing and/or allowing for greater active areas. In our model, current matching can be achieved by adjusting the GaAs absorber thickness. We modeled this condition, using today's utility-scale BOS parameters, and plot the results in Figure 3(b). Overall, the trajectory shifts away from the cost-competitive region when module costs are kept at \$45/m^2, which is a direct consequence of the GaAs thickness constraint required for current matching. Although thinning the GaAs layer to the required ~300 nm saves cell costs, the concurrent reduction in top cell efficiency overcompensates and increases system cost with respect to a single-junction GaAs module. We observe a similar trend for the residential-scale scenarios (not shown). The green squares illustrate the impact of reducing module assembly costs \$30/m^2. If module assembly cost savings are realized in this configuration, they should be around \$15/m^2 and more to compete with the single-junction alternatives.

The lack of tandem benefit relative to the single-junction III–V alternative is due to the Si bottom cell not contributing enough power to offset the cost of including it in the tandem. We thus considered whether a more efficient Si cell would give a substantially different result. We increased the silicon bottom cell's open-circuit voltage by 50 mV, such as might be achievable using advanced n-type cell technology, but the trajectory remains essentially unchanged (empty squares in Figure 3(b)), because the Si single-junction module is also more efficient. We also considered the favorable scenario where a 28.5% efficient GaAs module was combined with a 21.4% Si module, to produce a 36% efficient tandem module, while holding all other cost parameters constant. At minimum module cost, the silicon contributed about 7.5% to the total efficiency. As shown in the open squares in Figure 3(b), we again find that the cost trajectory does not change dramatically, due to the improved competitiveness of the highly efficient single junctions. We find similar trends for other BOS conditions.

5. InGaP/PERC Si TANDEM

In contrast to the GaAs/Si tandem, the InGaP and Si bandgaps are nearly ideally paired to maximize tandem efficiency [17]. Hence, the cost benefit, at the system level,

DOI: 10.1002/pip

from each cell is higher with respect to the GaAs/Si tandem. This ideal pairing nevertheless has only a small impact on the cost trajectories, shown in Figure 4. We also show where the InGaP BCC = Si BCC, indicated by the stars. Like the GaAs/Si case, the InGaP/Si tandem is broadly cost-competitive only in the space-constrained residential scenario and only when the InGaP BCC cost lies within the ranges indicated in Figure 4.

The maximum benefit is 7.5%, which is only slightly better than for GaAs/Si. After achieving substantial BOS reductions like those proposed by SunShot, the tandem remains cost-competitive over a limited range of III–V cell cost, but the system cost advantage of the tandem structure decreases to at most 2.5%.

Interestingly, in all cases we studied, the InGaP thickness that optimizes system cost is about 800 nm, whereas commonly studied InGaP devices for mechanical stacks are usually about 1-μm thick [4,13]. When constrained to 1 μm, the cost trajectory (not shown) is still potentially cost-competitive for today's residential systems, but offers even less cost advantage over single junctions.

6. CONCLUSIONS

A simple system cost model for III–V/Si tandem architectures was presented that accounts for variations in cost and efficiency related to cell thickness, which is a major cost driver for III–V solar cell technologies. The model simplifies system cost analysis by condensing typically complex cost structures into a few accessible parameters, which we tabulated based on available cost data from the literature. The data indicate that the cost-competitiveness for the III–V/Si tandem is essentially the same for GaAs/Si and GaInP/Si when considering the best-in-class performance of GaAs and GaInP cells to date. Both GaAs/Si and InGaP/Si tandems are potentially cost-competitive in scenarios where area-related BOS costs are high, like space-constrained residential applications, but the maximum reduction in system cost is less than 10%. The window of opportunity decreases as costs for either single junction decrease. III–V/Si tandems do not appear to be potentially cost-competitive for utility-scale applications, regardless of the III–V cell cost. This model can be applied to other emerging candidates for the top cell material, using our parameters, so long as a reasonable estimate of cell performance and cost versus thickness is known.

ACKNOWLEDGEMENTS

This work was supported by the U.S. Department of Energy under contract no. DE-AC36-08GO28308 with the National Renewable Energy Laboratory. Funding was provided by the DOE Office of Energy Efficiency and Renewable Energy Solar Energy Technologies Program under agreement number DE-EE00025784 for "PV Partnering & Business Development."

REFERENCES

1. Goodrich AC, Powell DM, James TL, Woodhouse M, Buonassisi T. Assessing the drivers of regional trends in solar photovoltaic manufacturing. *Energy and Environmental Science* 2013; **6**(10): 2811–2821.
2. Basore PA. Understanding manufacturing cost influence on future trends in silicon photovoltaics. *IEEE Journal of Photovoltaics* 2014; **4**(6): 1477–1482.
3. Goodrich A, Hacke P, Wang Q, Sopori B, Margolis R, James TL, Woodhouse M. A wafer-based monocrystalline silicon photovoltaics road map: utilizing known technology improvement opportunities for further reductions in manufacturing costs. *Solar Energy Materials and Solar Cells* 2013; **114**: 110–135.
4. Essig S. Progress towards a 30% efficient GaInP/Si tandem solar cell. *Energy Procedia* 2015; **77**: 464–469.
5. Tanabe K, Watanabe K, Arakawa Y. III–V/Si hybrid photonic devices by direct fusion bonding. *Scientific Reports* 2012; **2**: 349.
6. Woodhouse M, Goodrich A. A manufacturing cost analysis relevant to single and dual junction photovoltaic cells fabricated with III–Vs and III–Vs grown on Czochralski Silicon. PR-6A20-60126 92, 2013.
7. Ward S, Remo T, Horowitz K, Woodhouse M, Sopori B, VanSant K, Basore P. Techno-economic analysis of three different substrate removal and reuse strategies for III–V solar cells. Submitted to *Progress in Photovoltaics: Research and Applications* 2016.
8. Jones-Albertus R, Feldman D, Fu R, Horowitz K, Woodhouse M. Technology advances needed for photovoltaics to achieve widespread grid price parity. Submitted to *Progress in Photovoltaics: Research and Applications* 2016.
9. US Department of Energy, *SunShot Vision Study* 2012.
10. Powell DM, Winkler MT, Choi HJ, Simmons CB, Needleman DB, Buonassisi T. Crystalline silicon photovoltaics: a cost analysis framework for determining technology pathways to reach baseload electricity costs. *Energy and Environmental Science* 2012; **5**(3): 5874–5883.
11. Powell DM, Winkler MT, Goodrich A, Buonassisi T. Modeling the cost and minimum sustainable price of crystalline silicon photovoltaic manufacturing in the United States. *IEEE Journal of Photovoltaics* 2013; **3**(2): 662–668.
12. Clugston DA, Basore PA. PC1D version 5: 32-bit solar cell modeling on personal computers. 26th IEEE Photovoltaic Specialists Conference 1997: 207–210.

13. Geisz JF, Steiner MA, Garcia I, Kurtz SR, Friedman DJ. Enhanced external radiative efficiency for 20.8% efficient single-junction GaInP solar cells. *Applied Physics Letters* 2013; (4): 103.
14. Bauhuis GJ, Mulder P, Haverkamp EJ, Huijben JCCM, Schermer JJ. 26.1% thin-film GaAs solar cell using epitaxial lift-off. *Solar Energy Materials and Solar Cells* 2009; **93**(9): 1488–1491.
15. Pan N. Epitaxial lift-off of large-area GaAs multijunction solar cells for high efficiency clean and portable energy power generation. IEEE-ICSE2014 Proc. 2014.
16. Basore PA. Recommended method for using PC1D to model a tandem cell structure. www.pc2d.info, accessed September 2015.
17. Grassman TJ, Carlin, JA, Ratcliff C, Chmielewski DJ, Ringel SA. Epitaxially-grown metamorphic GaAsP/Si dual-junction solar cells, 39th IEEE Photovoltaic Specialists Conference 2013: 0149–0153.

DOI: 10.1002/pip